

Multi-hop Relay Networks with Multiple-antenna Equipped Source and Destination

Gayan Amarasuriya, Chintha Tellambura and Masoud Ardakani
 Department of Electrical and Computer Engineering,
 University of Alberta, Edmonton, AB, Canada T6G 2V4
 Email: {amarasur, chintha, ardakani}@ece.ualberta.ca

Abstract—The performance of a multi-hop amplify-and-forward relay network is analyzed. The source and destination terminals are equipped with multiple-antennas and the relays with single-antennas. The cumulative distribution function and the moment generating function of two tight upper bounds of the end-to-end signal-to-noise ratio are derived. The lower bounds for the outage probability and the average symbol error rate (SER) are also derived. The results take into account the source-relay and the relay-destination correlation matrices; the uncorrelated case is treated as well. The asymptotic outage probability, average SER, diversity order and coding gain are also derived. Numerical results and Monte-Carlo simulations are presented to analyze the system performance and show the tightness of the proposed bounds.

I. INTRODUCTION

In relay networks, the use of multiple antennas at the source (S) and the destination (D) significantly improves the performance [1]. Possible ways to utilize multiple antennas are transmit beamforming and receiver diversity combining [2], [3]. For example, beamforming, i.e., maximal ratio transmission (MRT) and maximal ratio combining (MRC) has been studied for several types of relay networks [4]–[8].

These studies [4]–[8] focus on dual-hop networks and the relay is limited to single antenna. In [4], the performance of MRT/MRC beamforming in dual-hop amplify-and-forward (AF) relay network with multiple-antenna S and D terminals over independent Rayleigh fading is studied. Reference [5] extends [4] by taking into account the channel correlation for the different antenna elements at S and D . Moreover, in [6], the performance of such networks with semi-blind (fixed-gain) relays over independent Nakagami- m fading is investigated. In [7] and [8], the impact of multiple antennas at S on the outage probability and the effect of feedback delays are investigated, respectively, for dual-hop systems using MRT for the source-to-relay channel.

In this paper, we extend [4] and [5] to multi-hop networks by considering a series (two or more) of single-antenna AF relays between S and D . Since multi-hop relaying extends the coverage, analyzing its performance is important. Unfortunately, the exact statistics of the end-to-end signal-to-noise ratio (SNR) of this system appears analytically intractable. We thus use the SNR upper bounds developed for multi-hop relay networks in [9], [10]. By using these upper bounds, the cumulative distribution function (CDF), the moment generation function (MGF), and lower bounds for the outage probability

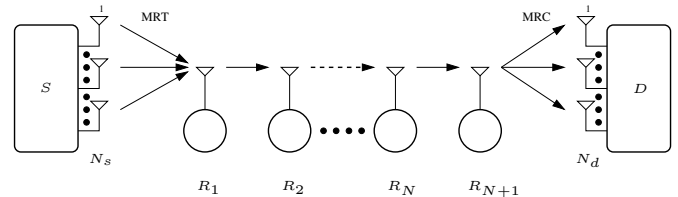


Fig. 1. Multi-hop relay network with multiple-antenna source-destination pair

and the average symbol error rate (SER) are derived. The results are sufficiently general to take into account the source-relay and the relay-destination correlation matrices. The performance metrics for the uncorrelated fading case are explicitly derived since they are not special cases of the correlated fading case. The asymptotic outage probability, average SER, diversity order and the coding gain are also derived. Moreover, the system performance is studied via numerical results and Monte-Carlo simulations.

The rest of this paper is organized as follows. Section II presents the system model. In Section III, the performance analysis is presented. Section IV contains the numerical and simulation results. Section V concludes the paper.

Notations: $\mathcal{K}_\nu(z)$ is the Modified Bessel function of the second kind of order ν [11, Eq. (8.407.1)]. ${}_2\mathcal{F}_1(\alpha, \beta; \gamma; z)$ is the Gauss Hypergeometric function [11, Eq. (9.14.1)].

II. SYSTEM MODEL

We consider a multi-hop relay network with MIMO-enabled S and D with N_s and N_d antennas, respectively. There are $N+1$ single-antenna AF relays $R_n|_{n=1}^{N+1}$ between S and D (Fig. 1). Perfect channel state information is assumed. The signal transmission from S takes the form of MRT, and the signal reception at D takes the form of MRC. The S - R_1 and R_{N+1} - D channels are arbitrary correlated Rayleigh fading with correlation matrices Ψ_S and Ψ_D , respectively. The R_n - R_{n+1} , $n = 1, \dots, N$, channels are independent and non-identically distributed (i.n.i.d.) Rayleigh fading.

Under this system model, the end-to-end SNR of a multi-hop ideal channel-assisted AF (CA-AF) relay network is given by [12]

$$\gamma_{CA} = \left[\frac{1}{\gamma_s} + \frac{1}{\gamma_d} + \sum_{n=1}^N \frac{1}{\gamma_n} \right]^{-1}, \quad (1)$$

where γ_s and γ_d are the instantaneous equivalent SNRs of the S - R_1 and R_{N+1} - D channels, respectively. The instantaneous SNR of the channel between R_n and R_{n+1} relays is denoted by γ_n . To analyze the system performance, the probability distributions of γ_{CA} in (1) are required, which is not mathematically tractable, particularly for $N > 1$. This problem can be overcome by using the SNR upper bounds γ_{eq}^{ub1} and γ_{eq}^{ub2} proposed in [9] and [10], respectively. They are given by

$$\gamma_{eq}^{ub1} = \min(\gamma_s, \gamma_d, \gamma_1, \gamma_2, \dots, \gamma_N), \quad \text{and} \quad (2)$$

$$\gamma_{eq}^{ub2} = \left[\frac{1}{\min(\gamma_s, \gamma_d)} + \frac{1}{\min(\gamma_1, \gamma_2, \dots, \gamma_N)} \right]^{-1}. \quad (3)$$

Reference [10] shows that γ_{eq}^{ub2} is always tighter than γ_{eq}^{ub1} in low-to-high SNRs and the asymptotically exactness of both bounds. Our performance analysis is based on (3). Because γ_{eq}^{ub1} yields simpler expressions for the performance metrics, the corresponding results for the γ_{eq}^{ub1} are also developed. Additional applications of the bounding technique (3) can be found in [10].

III. PERFORMANCE ANALYSIS

In this section, the statistics of the tighter SNR upper bound γ_{eq}^{ub2} are derived and then used to obtain the lower bounds for the outage probability and the average SER. The high SNR analysis of these performance metrics is presented to obtain valuable insights. The distribution functions and the performance metrics of γ_{eq}^{ub1} are also derived, as they are simpler than those of γ_{eq}^{ub2} .

A. Statistical characterization of the end-to-end SNR

The CDF of γ_{eq}^{ub2} when S and D experience correlated fading is given by (see the Appendix for the proof)

$$\begin{aligned} F_{\gamma_{eq}^{ub2}}(x) &= 1 - \sum_{j=1}^{N_s} \sum_{k=1}^{N_d} \frac{2(-1)^{j+k+N_s+N_d} \omega_j^{N_s-1} \lambda_k^{N_d-1}}{\Delta(\Psi_S)\Delta(\Psi_D)} \\ &\times \Delta_{N_s,j}(\mathcal{A}(\Psi_S))\Delta_{N_d,j}(\mathcal{A}(\Psi_D))\sqrt{\mu\nu_{j,k}} \\ &\times x e^{-x(\mu+\nu_{j,k})} \mathcal{K}_1(2x\sqrt{\mu\nu_{j,k}}). \end{aligned} \quad (4)$$

where $\mu = \sum_{n=1}^N \frac{1}{\tilde{\gamma}_n}$ and $\nu_{j,k} = \frac{\tilde{\gamma}_s \omega_j + \tilde{\gamma}_d \lambda_k}{\tilde{\gamma}_s \tilde{\gamma}_d \omega_j \lambda_k}$. Moreover, $\tilde{\gamma}_s$ and $\tilde{\gamma}_d$ are the equivalent average SNR of the S - R_1 and R_{N+1} - D channels. The average SNR of R_n - R_{n+1} channel is denoted by $\tilde{\gamma}_n$. Also $\omega_1 > \dots > \omega_{N_s}$ and $\lambda_1 > \dots > \lambda_{N_d}$ are the eigenvalues of Ψ_S and Ψ_D , respectively. $\Delta(\varphi)$ is the Vandermonde determinant of the eigenvalues of φ , and $\Delta_{m,j}(\mathcal{M})$ is the determinant of the matrix \mathcal{M} with the m -th row and j -th column removed. The (i, j) -th element of $\mathcal{A}(\mathcal{M})$ is given by $\mathcal{A}(\mathcal{M})_{i,j} = v_j^{i-1}$, where v denotes the eigenvalues of \mathcal{M} . The CDF of γ_{eq}^{ub1} is given by $F_{\gamma_{eq}^{ub1}}(x) = 1 - \sum_{j=1}^{N_s} \sum_{k=1}^{N_d} \frac{(-1)^{j+k+N_s+N_d} \omega_j^{N_s-1} \lambda_k^{N_d-1} \Delta_{N_s,j}(\mathcal{A}(\Psi_S))\Delta_{N_d,j}(\mathcal{A}(\Psi_D))}{\Delta(\Psi_S)\Delta(\Psi_D)} e^{-x(\mu+\nu_{j,k})}$.

The MGF of γ_{eq}^{ub2} when S and D experience correlated fading can be derived by substituting (4) into $M_{\gamma_{eq}^{ub2}}(s) = \int_0^\infty s F_{\gamma_{eq}^{ub2}}(x) e^{-sx} dx$, and evaluating the resulting integral by using [11, Eq. (6.621.3)] as follows:

$$\begin{aligned} M_{\gamma_{eq}^{ub2}}(s) &= 1 - \sum_{j=1}^{N_s} \sum_{k=1}^{N_d} \frac{16(-1)^{j+k+N_s+N_d} \omega_j^{N_s-1} \lambda_k^{N_d-1}}{3\Delta(\Psi_S)\Delta(\Psi_D)} \\ &\times \Delta_{N_s,j}(\mathcal{A}(\Psi_S))\Delta_{N_d,j}(\mathcal{A}(\Psi_D)) \mu \nu_{j,k} \\ &\times \frac{s {}_2F_1\left(3, \frac{3}{2}; \frac{5}{2}; \frac{s+\mu+\nu_{j,k}-2\sqrt{\mu\nu_{j,k}}}{s+\mu+\nu_{j,k}+2\sqrt{\mu\nu_{j,k}}}\right)}{(s+\mu+\nu_{j,k}+2\sqrt{\mu\nu_{j,k}})^3}. \end{aligned} \quad (5)$$

The corresponding MGF of γ_{eq}^{ub1} is given by $M_{\gamma_{eq}^{ub1}}(s) = 1 - \sum_{j=1}^{N_s} \sum_{k=1}^{N_d} \frac{(-1)^{j+k+N_s+N_d} \omega_j^{N_s-1} \lambda_k^{N_d-1} \Delta_{N_s,j}(\mathcal{A}(\Psi_S))\Delta_{N_d,j}(\mathcal{A}(\Psi_D))}{\Delta(\Psi_S)\Delta(\Psi_D)} \frac{1}{(s+\mu+\nu_{j,k})}$.

Remark 3.1: The case when S and D have uncorrelated antennas does not follow from (4) and (5) by replacing Ψ_S and Ψ_D with the identity matrix, because of the indeterminate $\frac{0}{0}$ form of the Vandermonde determinants. Thus, the CDF and the MGF for this case are explicitly derived.

The CDF of γ_{eq}^{ub2} when S and D experience uncorrelated fading is given by

$$\begin{aligned} F_{\gamma_{eq}^{ub2}}(x) &= 1 - \sum_{a=0}^{N_s-1} \sum_{b=0}^{N_d-1} \sum_{c=0}^{a+b} \frac{2}{\tilde{\gamma}_s^a \tilde{\gamma}_d^b a! b!} \binom{a+b}{c} \frac{\nu^{\frac{c-a-b+1}{2}}}{\mu^{\frac{c-a-b-1}{2}}} \\ &\times x^{a+b+1} e^{-x(\mu+\nu)} \mathcal{K}_{c-a-b+1}(2x\sqrt{\mu\nu}), \end{aligned} \quad (6)$$

where $\mu = \sum_{n=1}^N \frac{1}{\tilde{\gamma}_n}$ and $\nu = \frac{\tilde{\gamma}_s + \tilde{\gamma}_d}{\tilde{\gamma}_s \tilde{\gamma}_d}$, respectively. The CDF of γ_{eq}^{ub1} is given by $F_{\gamma_{eq}^{ub1}}(x) = 1 - \sum_{a=0}^{N_s-1} \sum_{b=0}^{N_d-1} \frac{1}{\tilde{\gamma}_s^a \tilde{\gamma}_d^b a! b!} x^{a+b} e^{-x(\mu+\nu)}$.

The MGF of γ_{eq}^{ub2} for this case can then be derived as

$$\begin{aligned} M_{\gamma_{eq}^{ub2}}(s) &= 1 - \sum_{a=0}^{N_s-1} \sum_{b=0}^{N_d-1} \sum_{c=0}^{a+b} \frac{2\sqrt{\pi}\mu(4\nu)^{c-a-b+1}}{\tilde{\gamma}_s^a \tilde{\gamma}_d^b a! b!} \binom{a+b}{c} \\ &\times \frac{\Gamma(c+3)\Gamma(2a+2b-c+1)}{\Gamma(a+b+\frac{5}{2})} \\ &\times \frac{s {}_2F_1\left(c+3, c-a-b+\frac{3}{2}; a+b+\frac{5}{2}; \theta(s)\right)}{(s+\mu+\nu+2\sqrt{\mu\nu})^{c+3}}, \end{aligned} \quad (7)$$

where $\theta(s) = \frac{s+\mu+\nu-2\sqrt{\mu\nu}}{s+\mu+\nu+2\sqrt{\mu\nu}}$. The corresponding MGF of γ_{eq}^{ub1} is given by $M_{\gamma_{eq}^{ub1}}(s) = 1 - \sum_{a=0}^{N_s-1} \sum_{b=0}^{N_d-1} \frac{s\Gamma(a+b+1)}{\tilde{\gamma}_s^a \tilde{\gamma}_d^b a! b!(s+\mu+\nu_{j,k})}$.

The probability density function (PDF) of $\gamma_{eq}^{ubi}|_{i=1}^2$ can easily be derived by differentiating CDFs of $\gamma_{eq}^{ubi}|_{i=1}^2$ with respect to x and by using $x \frac{\partial \mathcal{K}_\nu(x)}{\partial x} + \nu \mathcal{K}_\nu(x) + x \mathcal{K}_{\nu-1}(x) = 0$ [11, Eq. (8.486.12)]. However, for the sake of brevity, the PDF results are omitted.

B. Outage probability

The outage probability is the probability that the end-to-end instantaneous SNR falls below a predefined threshold γ_{th} . Hence, it is obtained as follows:

$$P_{out}^{lb} = \Pr(0 \leq \gamma_{eq}^{ub} \leq \gamma_{th}) = F_{\gamma_{eq}^{ub}}(\gamma_{th}). \quad (8)$$

C. Average error rate

The average SER is derived by integrating the conditional error probability (CEP) $P_e|\gamma$ over the PDF of the SNR. For certain commonly used modulation schemes, the CEP has the form; $P_e|\gamma = \alpha \mathcal{Q}(\sqrt{\beta\gamma})$, where α and β are constants dependent on the modulation scheme. The average SER has the integral representation $\bar{P}_e = \frac{\alpha}{2} - \frac{\alpha}{2} \sqrt{\frac{\beta}{2\pi}} \int_0^\infty x^{-\frac{1}{2}} e^{-\frac{\beta x}{2}} (1 - F_{\gamma_{eq}}(x)) dx$ [4]. By substituting (4) into \bar{P}_e and evaluating the resulting integral by using [11, Eq. (6.621.3)], a lower bounds for the average SER obtained by using γ_{eq}^{ub2} is derived as follows:

$$\begin{aligned} \bar{P}_e^{lb2} &= \frac{\alpha}{2} - \sqrt{\frac{\beta}{2}} \sum_{j=1}^{N_s} \sum_{k=1}^{N_d} \frac{3\alpha\pi(-1)^{j+k+N_s+N_d}\mu\nu_{j,k}}{\Delta(\Psi_S)\Delta(\Psi_D)} \\ &\times \omega_j^{N_s-1} \lambda_k^{N_d-1} \Delta_{N_s,j}(\mathcal{A}(\Psi_S)) \Delta_{N_d,j}(\mathcal{A}(\Psi_D)) \\ &\times \frac{{}_2\mathcal{F}_1\left(\frac{5}{2}, \frac{3}{2}; 2; \frac{\frac{\beta}{2} + \mu + \nu_{j,k} - 2\sqrt{\mu\nu_{j,k}}}{\frac{\beta}{2} + \mu + \nu_{j,k} + 2\sqrt{\mu\nu_{j,k}}}\right)}{\left(\frac{\beta}{2} + \mu + \nu_{j,k} + 2\sqrt{\mu\nu_{j,k}}\right)^{\frac{5}{2}}}. \end{aligned} \quad (9)$$

The average SER with γ_{eq}^{ub1} is given by

$$\bar{P}_e^{lb2} = \frac{\alpha}{2} - \frac{\alpha}{2} \sqrt{\frac{\beta}{2}} \sum_{j=1}^{N_s} \sum_{k=1}^{N_d} (-1)^{j+k+N_s+N_d} \omega_j^{N_s-1} \lambda_k^{N_d-1} \frac{\Delta_{N_s,j}(\mathcal{A}(\Psi_S)) \Delta_{N_d,j}(\mathcal{A}(\Psi_D))}{\Delta(\Psi_S)\Delta(\Psi_D)\left(\frac{\beta}{2} + \mu + \nu_{j,k}\right)^{\frac{1}{2}}}.$$

As per Remark 3.1, the average SER for the uncorrelated case is explicitly derived. The lower bounds for the average SER obtained by using γ_{eq}^{ub2} for this case is given by

$$\begin{aligned} \bar{P}_e^{lb2} &= \frac{\alpha}{2} - \alpha \sqrt{\frac{\beta}{2}} \sum_{a=0}^{N_s-1} \sum_{b=0}^{N_d-1} \sum_{c=0}^{a+b} \frac{\mu(4\nu)^{c-a-b+1}}{\bar{\gamma}_s^a \bar{\gamma}_d^b a! b!} \binom{a+b}{c} \\ &\times \frac{\Gamma(c + \frac{5}{2}) \Gamma(2a + 2b - c + \frac{1}{2})}{\Gamma(a + b + 2)} \\ &\times \frac{{}_2\mathcal{F}_1\left(c + \frac{5}{2}, c - a - b + \frac{3}{2}; a + b + 2; \theta(\beta/2)\right)}{\left(\frac{\beta}{2} + \mu + \nu + 2\sqrt{\mu\nu}\right)^{c + \frac{5}{2}}}. \end{aligned} \quad (10)$$

The corresponding average SER for γ_{eq}^{ub1} is given by $\bar{P}_e^{lb1} = \frac{\alpha}{2} - \frac{\alpha}{2} \sqrt{\frac{\beta}{2\pi}} \sum_{a=0}^{N_s-1} \sum_{b=0}^{N_d-1} \frac{\Gamma(a+b+\frac{1}{2})}{\bar{\gamma}_s^a \bar{\gamma}_d^b a! b! \left(\frac{\beta}{2} + \mu + \nu\right)^{a+b+\frac{1}{2}}}.$

D. High SNR Analysis

In this section, the asymptotic outage probability, the average SER, the coding gain and the diversity gain are derived. Our asymptotic results hold for both γ_{eq}^{ub1} and γ_{eq}^{ub2} bounds as the performance metrics derived by using them are asymptotically exact [10].

1) *Asymptotic outage probability*: The asymptotic outage probability when S and D experience correlated fading can be derived as follows: The behavior of the CDF of γ_{eq}^{ub2} for a large $\bar{\gamma}$ is equivalent to the behavior of $F_{\gamma_{eq}^{ub2}}(y)$ around $y = 0$ [13]. By substituting $\bar{\gamma}_n|_{n=1}^N = C_n \bar{\gamma}$, $\gamma_d = C_d \bar{\gamma}$, $\gamma_s = C_s \bar{\gamma}$ and $x = \bar{\gamma}y$ into (4), and by expressing the exponential function and Bessel function in terms of their Taylor series expansions around $y = 0$ [11, Eq. (1.211) and Eq. (8.446)], the expression with the first order terms of y can be obtained. Then the asymptotic outage probability can be obtained by substituting $y = \frac{\gamma_{th}}{\bar{\gamma}}$ as follows:

$$P_{out}^\infty = F_{\gamma_{eq}^{ub}}^\infty(\gamma_{th}) = \Omega_0 \frac{\gamma_{th}}{\bar{\gamma}} + o\left(\frac{\gamma_{th}}{\bar{\gamma}}\right)^2, \quad \text{where} \quad (11)$$

$$\begin{aligned} \Omega_0 &= \sum_{j=1}^{N_s} \sum_{k=1}^{N_d} \frac{(-1)^{j+k+N_s+N_d} \omega_j^{N_s-1} \lambda_k^{N_d-1}}{\Delta(\Psi_S)\Delta(\Psi_D)} \\ &\times \Delta_{N_s,j}(\mathcal{A}(\Psi_S)) \Delta_{N_d,j}(\mathcal{A}(\Psi_D)) \\ &\times \left(\sum_{n=1}^N \frac{1}{C_n} + \frac{1}{C_s \omega_j} + \frac{1}{C_d \lambda_k} \right), \\ C_n|_{n=1}^N &= \frac{\bar{\gamma}_n}{\bar{\gamma}}, \quad C_s = \frac{\bar{\gamma}_s}{\bar{\gamma}} \quad \text{and} \quad C_d = \frac{\bar{\gamma}_d}{\bar{\gamma}}. \end{aligned} \quad (12)$$

The asymptotic outage probability when S and D experience uncorrelated fading is given by

$$P_{out}^\infty = \begin{cases} \Omega_1 \frac{\gamma_{th}}{\bar{\gamma}} + o\left(\frac{\gamma_{th}}{\bar{\gamma}}\right)^2, & N_s = N_d = 1 \\ \Omega_2 \frac{\gamma_{th}}{\bar{\gamma}} + o\left(\frac{\gamma_{th}}{\bar{\gamma}}\right)^2, & N_s = 1 \quad \text{and} \quad N_d > 1 \\ \Omega_3 \frac{\gamma_{th}}{\bar{\gamma}} + o\left(\frac{\gamma_{th}}{\bar{\gamma}}\right)^2, & N_s > 1 \quad \text{and} \quad N_d = 1 \\ \Omega_4 \frac{\gamma_{th}}{\bar{\gamma}} + o\left(\frac{\gamma_{th}}{\bar{\gamma}}\right)^2, & N_s > 1 \quad \text{and} \quad N_d > 1, \end{cases} \quad (13)$$

where $\Omega_1 = \frac{1}{C_s} + \frac{1}{C_d} + \sum_{n=1}^N \frac{1}{C_n}$, $\Omega_2 = \frac{1}{C_s} + \sum_{n=1}^N \frac{1}{C_n}$, $\Omega_3 = \frac{1}{C_d} + \sum_{n=1}^N \frac{1}{C_n}$, and $\Omega_4 = \sum_{n=1}^N \frac{1}{C_n}$.

2) *Asymptotic average SER*: The average SER at high SNR can be derived by substituting (11) and (13) into the integral representation of SER in Section III-C and then solving it as; $\bar{P}_e^\infty = \frac{\Omega\alpha}{2\beta\bar{\gamma}} + o(\bar{\gamma}^{-2})$. The asymptotic average SER for the correlated fading case can be obtained by replacing Ω by Ω_0 . The asymptotic average SER for each cases in (13) of the uncorrelated fading case can be obtained by replacing Ω by Ω_1 , Ω_2 , Ω_3 and Ω_4 . In the high SNR regime, the average SER can be represented by $\bar{P}_e^\infty \approx [G_c \bar{\gamma}]^{-G_d}$, where G_d and G_c are referred to as the diversity gain and coding gain, respectively [13]. Then, by using \bar{P}_e^∞ , the G_d and G_c can easily be obtained for each case. In [4], the diversity gain is given by the minimum number of antennas at S and D ; i.e., $G_d = \min(N_s, N_d)$. However, the diversity gain G_d of our set-up is one because it is governed by the $R_n - R_{n+1}|_{n=1}^N$ hops, which has only single-antenna terminals. Although this set-up is limited in terms of its achievable diversity order, the coverage can be extended considerably.

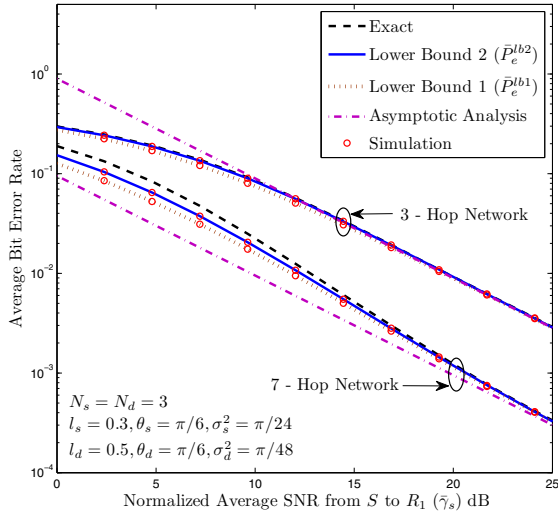


Fig. 2. The average BER of BPSK for 3-hop, and 7-hop relay networks. $d_{SD} = 1$ and $\eta = 2.5$. For the 3-hop network, $d_1 = 0.3, d_2 = 0.5$ and $d_3 = 0.2$. For the 7-hop network, $d_1 = 0.3, d_2 = 0.1, d_3 = 0.15, d_4 = 0.05, d_5 = 0.1, d_6 = 0.1$ and $d_7 = 0.2$.

IV. NUMERICAL RESULTS

This section presents numerical and simulation results in order to investigate the performance of our bounds, and to verify the analytical results of Section III. The average SNR of the i -th hop is modeled by $\bar{\gamma}_i = \bar{\gamma} \left(\frac{d_{SD}}{d_i} \right)^\eta$, where $\bar{\gamma}$ and η are the reference average SNR and path-loss exponent. The distance between the source-destination pair is d_{SD} and that between R_i and R_{i+1} is d_i . The correlation matrices Ψ_S and Ψ_D for uniform linear antenna arrays at S and D are constructed using [14, Eq. (4)]. The amount of spatial correlation between adjacent antenna elements then can be quantified by their relative antenna spacing (l_s, l_d), angular spreads (σ_s^2, σ_d^2), and the angle of arrival or departure (θ_s, θ_d).

1) *The impact of the number of hops on the average BER:* In Fig. 2, the average bit error rate (BER) of binary phase shift keying (BPSK) is plotted against the average SNR of the first hop for 3-hop, and 7-hop relay networks. S and D each uses three antennas ($N_s = N_d = 3$). Further, the asymptotic average BER curves are plotted. Fig. 2 shows that the average BER derived by using γ_{eq}^{ub2} is tighter than that of γ_{eq}^{ub1} in low-to-moderately high SNRs. For the 3-hop case, the proposed BER lower bound almost matches with the exact BER. However, as the number of hops increases, our bounds weaken for low SNRs. Further, this figure clearly reveals the performance benefits reaped by going from three-hops to seven-hops. The asymptotic analysis shows that our proposed bounds are exact for high SNR. Further, the Monte-Carlo results validate our analysis.

2) *The impact of correlated fading at S and D on the outage probability:* In Fig. 3, the outage probability is plotted for a 4-hop relay network. Two antenna setups (i) $N_s = N_d = 3$ and (ii) $N_s = N_d = 1$ are considered. Three different correlation scenarios are obtained as (a) high correlation:

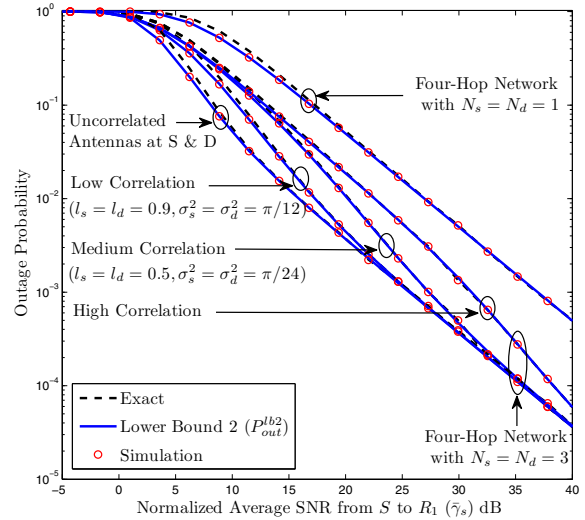


Fig. 3. The impact of antenna correlation at the source and the destination on the outage probability. $d_{SD} = 1$ and $\eta = 2.5$. $\theta_s = \theta_d = \pi/6$. $d_1 = 0.3, d_2 = 0.35, d_3 = 0.15$ and $d_4 = 0.2$.

($l_s = l_d = 0.2, \sigma_s^2 = \sigma_d^2 = \pi/48$), (b) medium correlation: ($l_s = l_d = 0.5, \sigma_s^2 = \sigma_d^2 = \pi/24$) and (c) low correlation: ($l_s = l_d = 0.9, \sigma_s^2 = \sigma_d^2 = \pi/12$). Since l_s and l_d are the relative antenna spacing, and σ_s^2 and σ_d^2 are the angular spread at S and D , respectively, smaller values of l_s, l_d, σ_s^2 and σ_d^2 result in higher spatial correlation [14]. The higher correlation effects at both S and D degrade the outage probability performance significantly. Fig. 3 also reveals that the outage probability improves as the number of antennas at S and D increases. Despite no diversity advantages¹, significant coding gains can be achieved by using multiple-antenna source-destination pair in multi-hop relay networks. The coding gain of antenna setup (ii) over setup (i) is about 15 dB.

3) *The impact of the number of antennas at S and D on the outage probability:* In Fig. 4, the outage probability for a 4-hop relay network is plotted for four different antenna configurations at S and D in i.i.i.d Rayleigh fading. The outage probability improves as the number of antennas at S and D increases. Although there are no diversity gains, the coding gain obtained by going from $N_s = N_d = 1$ to $N_s = N_d = 2$ is about 10 dB. However, further increase of antennas at S and D does not increase the coding gain. These results suggest that the use of two antennas at S and D is the best. This insight is also provided in Section III-D2, where the coding gain is independent of $\bar{\gamma}_s$ and $\bar{\gamma}_d$ as $N_s > 1$ and $N_d > 1$.

4) *The impact of the antenna spacing and angular spread at S and D on the average BER:* In Fig. 5, the impact of the antenna spacing at both S and D antennas on the average BER is depicted. Here a three-hop relay network is considered. Lower antenna spacing leads to higher antenna correlation and degrades the BER performance significantly. Moreover, lower angular spreads further weaken the BER performance.

¹The single-antenna relays limit the diversity order of the system to one.

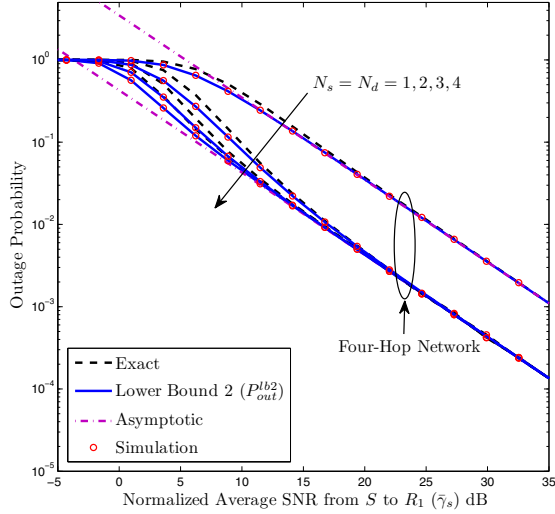


Fig. 4. The outage probability of four-hop relay network with different antenna configuration at the source and the destination. $d_{SD} = 1$ and $\eta = 2.5$. $d_1 = 0.3, d_2 = 0.4, d_3 = 0.1$, and $d_4 = 0.2$.

V. CONCLUSION

This paper presented a performance analysis of a multi-hop single-antenna AF relay networks with multiple-antenna S and D terminals. The CDF and the MGF were derived for two upper bounds of the end-to-end SNR. Lower bounds for the outage probability and the average SER were derived as well. The asymptotic outage probability and average SER, diversity order and coding gains were derived. The results show that the spatial correlation degrades the system performance considerably in a moderately high SNR regime, but that the degradation is much less pronounced in very low and very high SNR regimes. Moreover, a higher antenna separation and higher angular spreads reduce the impact of antenna correlation. Our bounds are tight in the moderate-to-high SNR regime and they are asymptotically exact. Our performance metrics can be useful as benchmarks for the design of MIMO multi-hop relay networks.

VI. APPENDIX

The CDF of $\gamma_{\text{eq}}^{\text{ub1}}|_{i=1}^2$ with channel correlation at S and D can be derived as follows: Let $\gamma_{\text{eq}}^{\text{ub1}} = \min(\gamma_s, \gamma_d, \gamma_1, \gamma_2, \dots, \gamma_N)$ and $\gamma_{\text{eq}}^{\text{ub2}} = \frac{\Gamma_1 \Gamma_2}{\Gamma_1 + \Gamma_2}$, where $\Gamma_1 = \min(\gamma_s, \gamma_d)$ and $\Gamma_2 = \min(\gamma_1, \gamma_2, \dots, \gamma_N)$. Then the complementary cumulative distribution function (CCDF) of Γ_1 can be obtained as $\bar{F}_{\Gamma_1}(x) = \bar{F}_{\gamma_s}(x) \bar{F}_{\gamma_d}(x)$, where $\bar{F}_{\gamma_s}(x) = \frac{1}{\Delta(\Psi_S)} \sum_{j=1}^{N_s} (-1)^{j+N_s} \omega_j^{N_s-1} \Delta_{N_s,j}(A(\Psi_S)) e^{-\frac{x}{\bar{\gamma}_s \omega_j}}$ and $\bar{F}_{\gamma_d}(x) = \frac{1}{\Delta(\Psi_D)} \sum_{k=1}^{N_d} (-1)^{k+N_d} \lambda_k^{N_d-1} \Delta_{N_d,k}(A(\Psi_D)) e^{-\frac{x}{\bar{\gamma}_d \lambda_k}}$ are the CCDFs of γ_s and γ_d , respectively [5]. The PDF of Γ_2 is given by $f_{\Gamma_2}(x) = \left[\sum_{n=1}^N \frac{1}{\bar{\gamma}_n} \right] \exp\left(-x \sum_{n=1}^N \frac{1}{\bar{\gamma}_n}\right)$. The CDF of $\gamma_{\text{eq}}^{\text{ub2}}$ (4) can readily be derived by substituting the CCDF of Γ_1 and PDF of Γ_2 into $F_{\gamma_{\text{eq}}^{\text{ub2}}}(x) = 1 - \int_0^\infty \bar{F}_{\Gamma_1}\left(\frac{(z+x)x}{z}\right) f_{\Gamma_2}(z+x) dz$ and evaluating the resulting integral by using [11, Eq. (3.471.9)]. The CDF of $\gamma_{\text{eq}}^{\text{ub1}}$ can be obtained by $F_{\gamma_{\text{eq}}^{\text{ub1}}}(x) = 1 - \bar{F}_{\gamma_s}(x) \bar{F}_{\gamma_d}(x) \bar{F}_{\Gamma_2}(x)$.

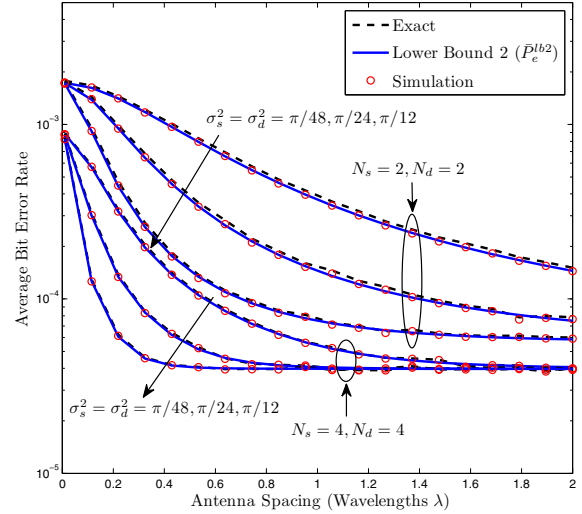


Fig. 5. The impact of antenna spacing and angular spread at the source and destination on the average BER of BPSK. $\theta_s = \theta_d = \pi/6$, $d_{SD} = 1$ and $\eta = 2.5$. $d_1 = 0.45, d_2 = 0.1$ and $d_3 = 0.45$.

REFERENCES

- [1] Y. Fan and J. Thompson, "MIMO configurations for relay channels: Theory and practice," *IEEE Trans. Wireless Commun.*, vol. 6, no. 5, pp. 1774–1786, May 2007.
- [2] T. K. Y. Lo, "Maximum ratio transmission," *IEEE Trans. Commun.*, vol. 47, no. 10, pp. 1458–1461, Oct. 1999.
- [3] P. Digham, R. Mallik, and S. Jamuar, "Analysis of transmit-receive diversity in Rayleigh fading," *IEEE Trans. Commun.*, vol. 51, no. 4, pp. 694–703, April 2003.
- [4] R. H. Y. Louie, Y. Li, and B. Vucetic, "Performance analysis of beamforming in two hop amplify and forward relay networks," in *Proc. IEEE International Conference on Communications*, May 19–23, 2008, pp. 4311–4315.
- [5] R. Louie, Y. Li, H. Suraweera, and B. Vucetic, "Performance analysis of beamforming in two hop amplify and forward relay networks with antenna correlation," *IEEE Trans. Wireless Commun.*, vol. 8, no. 6, pp. 3132–3141, Jun. 2009.
- [6] D. da Costa and S. Aissa, "Cooperative dual-hop relaying systems with beamforming over Nakagami- m fading channels," *IEEE Trans. Wireless Commun.*, vol. 8, no. 8, pp. 3950–3954, August 2009.
- [7] H. Min, S. Lee, K. Kwak, and D. Hong, "Effect of multiple antennas at the source on outage probability for amplify-and-forward relaying systems," *IEEE Trans. Wireless Commun.*, vol. 8, no. 2, pp. 633–637, Feb. 2009.
- [8] H. A. Suraweera, T. A. Tsiftsis, G. K. Karagiannidis, and M. Faulkner, "Effect of feedback delay on downlink amplify-and-forward relaying with beamforming," in *IEEE Global Telecommunications Conference*, Dec. 2009.
- [9] M. O. Hasna, "Average BER of multihop communication systems over fading channels," in *10th IEEE International Conference on Electronics, Circuits and Systems ICECS*, vol. 2, Dec. 2003, pp. 723–726.
- [10] G. Amarasuriya, C. Tellambura, and M. Ardakani, "Asymptotically-exact performance bounds of AF multi-hop relaying over Nakagami fading," *IEEE Trans. Commun.*, 2009, (submitted).
- [11] I. Gradshteyn and I. Ryzhik, *Table of Integrals, Series, and Products*, 7th ed. Academic Press, 2000.
- [12] M. O. Hasna and M. S. Alouini, "Outage probability of multihop transmission over Nakagami fading channels," *IEEE Commun. Lett.*, vol. 7, no. 5, pp. 216–218, May 2003.
- [13] Z. Wang and G. B. Giannakis, "A simple and general parameterization quantifying performance in fading channels," *IEEE Trans. Commun.*, vol. 51, no. 8, pp. 1389–1398, Aug. 2003.
- [14] H. Bolcskei, M. Borgmann, and A. J. Paulraj, "Impact of the propagation environment on the performance of space-frequency coded MIMO-OFDM," *IEEE J. Sel. Areas Commun.*, vol. 21, no. 3, pp. 427–439, Apr. 2003.